MODELING DIFFERENTLY ORIENTED LOBLOLLY PINE STRANDS INCORPORATING VARIATION OF INTRARING PROPERTIES USING A STOCHASTIC FINITE ELEMENT METHOD

Gi Young Jeong

Postdoctoral Associate
Sustainable Engineered Material Institute
Virginia Polytechnic Institute and State University
230 Cheatham Hall
Blacksburg, VA 24061-0503

*Daniel P. Hindman**†*

Assistant Professor
Department of Wood Science and Forest Products
Virginia Polytechnic Institute and State University
Brooks Forest Products Center
1650 Ramble Road
Blacksburg, VA 24061-0503

(Received May 2009)

Abstract. Wood strands are a biological material with variations in material properties because of the presence of earlywood and latewood, juvenile wood and mature wood as well as the sectional cut used to generate strands. This variation should be accounted for to produce reliable modeling results. This study used both a deterministic finite element method (FEM) and a stochastic finite element method (SFEM) to model the stiffness of wood strands from three different orientations (radial, tangential, and angled) incorporating intraring property variation from two growth ring positions. In addition, a homogeneous model was used as a control to compare the results from both deterministic FEM and SFEM. The homogeneous model predicted the stiffness well for radial and tangential orientation strands but provided unrealistic physical strain distributions. Assumptions of strand homogeneity oversimplified the strain distribution present in the strand, eliminating local maximum and minimum values. Cumulative probability curves comparing previous experimental results and SFEM results showed general agreement. Average differences in the effective tensile modulus of elasticity ranged 0.96 – 22.31%. Based on the modeling results, the earlywood tensile modulus of elasticity was the input parameter that had the greatest influence on the strand stiffness. The order of correlation of the earlywood and latewood Poisson ratios changed based on strand orientation. SFEM techniques provided accurate results and material property distributions as compared with the experimental results.

Keywords: Stochastic finite element method (SFEM), Strands, modulus of elasticity (MOE), earlywood, latewood.

INTRODUCTION

Wood strands represent complex structures with many differences in possible anatomical configurations. As wood material is located further away from the pith, characteristics of cellular structures change from juvenile to mature wood. Juvenile wood contains higher microfibril angle, a greater percentage of compression wood, distorted grain patterns, and a lower percentage of latewood compared with mature wood (Larson et al 2001). Previous studies have shown that the tensile modulus of elasticity (MOE) of latewood is approximately twice that of earlywood (Groom et al 2002; Mott et al 2002; Cramer et al 2005). Variations of material properties of earlywood and latewood have also been found in different growth ring positions (Cramer et al 2005; Jeong et al 2009).

* Corresponding author: dhindman@vt.edu
† SWST member

To generate rigorous data of earlywood and latewood properties, Jeong et al (2009) measured the mechanical properties of earlywood and latewood samples of loblolly pine (*Pinus taeda*) from growth ring numbers 1 – 10 and 11 – 20 using tension testing incorporating digital image correlation for strain measurement. Tensile MOE and Poisson ratio increased as the growth ring number increased. Statistical comparisons showed that the tensile MOE and ultimate tensile strength (UTS) had a significant difference for both growth ring and intraring positions. Probability density functions for tensile MOE, Poisson ratios, and UTS were presented.

Jeong (2008) also measured the tensile properties of differently oriented loblolly pine strands from growth ring numbers 1 – 10 and 11 – 20. Tensile MOE and UTS of radial-, tangential-, and angled-oriented strands increased as growth ring number increased. Statistical comparisons showed that the growth ring position and cutting angle impacted the mechanical properties of the wood strands. Different failure modes were found for differently oriented strands because of different stress distributions in earlywood and latewood.

Successful strand modeling requires the measurement of the range of earlywood and latewood layers along with an accurate geometric configuration of these layers. Hindman and Lee (2007) constructed cellular and solid finite element method (FEM) models to predict the tensile MOE of differently oriented strands from loblolly pine under tensile and bending loading. The inputs for the models were average longitudinal elastic moduli of earlywood and latewood from experimental testing. Cellular models predicted experimental results ranging from 1.7 – 20.4% different from FEM models.

However, these models did not incorporate the variation of earlywood and latewood properties throughout the stem and the variation of material properties in wood strands. Material properties in wood can be considered as random variables with specific statistical distributions. Investigating the effect of these random variables can provide more accurate results for the mechanical properties of wood strands and consequently wood strand-based composites.

A useful tool that incorporates mechanical modeling and statistical property distributions is the stochastic finite element method (SFEM). SFEM computes the stochastic field of nodal displacements based on a random stiffness matrix (Kleiber and Hien 1992). SFEM takes advantage of existing FEM models combined with uncertainty variables using one of a variety of stochastic methods, including perturbation, Monte Carlo simulation, Neumann expansion, and Karhunen-Loeve decomposition. Previous authors, including Wang and Lam (1998, Clouston and Lam (2002), and Clouston (2007), have applied SFEM methods to predict mechanical properties of wood composites, but SFEM has not been previously applied to wood strands.

The goal of this work was to incorporate the effects of intraring properties and orientation of earlywood and latewood in wood strands into a model of the effective tensile MOE of wood strands. Monte Carlo simulation-based SFEM used the results from the earlywood and latewood testing (Jeong et al 2009) as inputs to model the mechanical property variation of loblolly pine wood strands. Validation of the SFEM model was determined by comparing the mechanical properties measured from wood strands of different orientations (Jeong 2008). The strain distribution across the width of the strand was examined. A correlation of the input parameters compared with predicted effective strand tensile MOE was also conducted.

METHODS

Differently Oriented Strand Models

Two-dimensional FEM and SFEM models for differently oriented strands from growth ring numbers 1 – 10 and 11 – 20 were constructed using an ANSYS 11.0v program. Both FEM and SFEM used the same mesh and the plane-183 elements from ANSYS. The plane stress option

was applied where the thickness of the model was used for stress and strain calculations.

The following assumptions were made for all models:

- Wood strands behaved in a linear elastic manner.
- No slippage occurred between earlywood and latewood under uniform loading.
- Applied load is constant (deterministic).

Figure 1 shows the four different wood strand meshes, dimensions, and the loading conditions of the models. Models include radially oriented (RO), tangentially oriented (TO), angled-oriented (AO), and homogeneous (H). The three orientations represent three different patterns of variations of earlywood and latewood properties, whereas the homogenous model does not include intraring property variations. For the TO model, the representative geometry of earlywood and latewood bands was created by cutting a tangent to the earlywood and latewood boundary when the wood disk assumed a tapered cylinder. All models were 100 mm long, 25.4 mm wide, and 0.6 mm thick. A uniformly distributed tension load was applied at the top of the strand with the bottom of the strand fixed in both x and y directions.

Convergence checks were conducted with a series of grids (coarse, medium, fine, and superfine). Convergence checks of all models produced stress and strain values with a difference of less than 1%. The number of elements

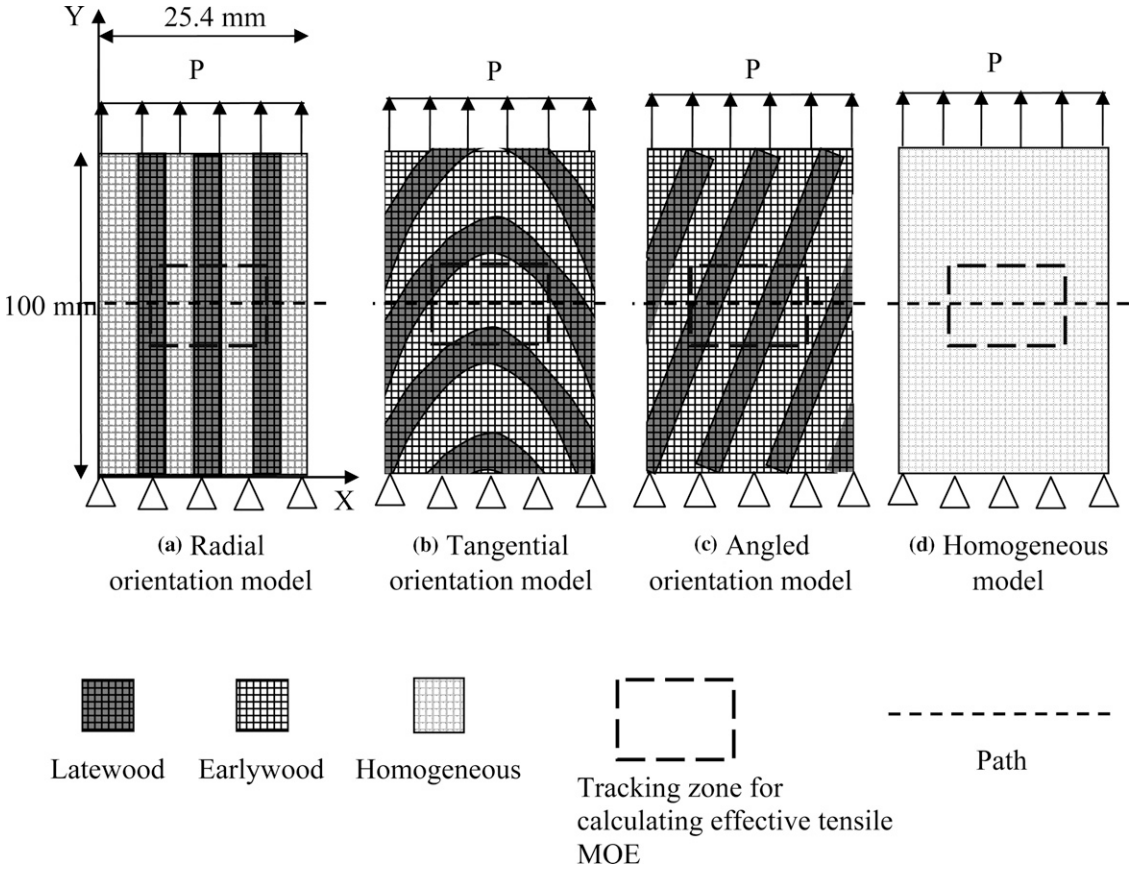

Figure 1. Structural analog of strand orientation models; (a) radial orientation model, (b) tangential orientation model, (c) angled orientation model, and (d) homogeneous model.

used were 2900 (R), 14683 (T), 4187 (A), and 2600 (H). Different element numbers for the different strand models were assigned based on the results of the convergence checks (Jeong 2005). Also, a patch test was conducted to check the connectivity of elements for each model.

Model Input Property Generation

Earlywood and latewood were defined as transverse isotropic materials considering in-plane properties only. Table 1 shows the statistical distribution type and parameters for the longitudinal modulus (E_L) and Poisson ratio (υ_{LR}) of earlywood and latewood from growth rings 1 – 10 and 11 – 20 from Jeong et al (2009).

The transverse elastic modulus (E_R) and in-plane shear modulus (G_{LR}) were calculated based on reciprocal relationships previously determined for strands. The ratio of E_L:E_R for earlywood and latewood from the two different growth ring positions was calculated by Jeong (2008). An E_L:E_R ratio of 2.72:1.0 was used for earlywood and latewood from growth ring numbers 1 – 10 and an $E_{L\ R}$ ratio of 3.12:1.0 for earlywood and latewood from growth ring numbers 11 – 20. Kretschmann et al (2006) found the ratio of E_L:G_{LR} for latewood and for earlywood was 3.5:1.0 regardless of growth ring position.

All deterministic FEM models except for the H model used the average E_L and υ_{LR} of earlywood and latewood from the two growth ring numbers, respectively. For the H model, average E_L and υ_{LR} values for the two growth ring numbers were calculated using the rule of mixtures based on an earlywood to latewood ratio of 2.0:1.0.

For probabilistic SFEM, a Monte Carlo simulation associated with the Latin Hypercube Sampling technique in the ANSYS 11.0v program was used to generate random earlywood and latewood properties based on the distribution type and distribution parameters (Table 1). The random earlywood and latewood properties were distributed on discretized meshes within the earlywood and latewood layers. One thousand analysis loops were executed to compute the distributed outputs as a function of the thousand sets of random input variables. One thousand loops were determined after the convergence check of mean and standard deviation using four different series of loops. The 1000 simulations for SFEM were deemed sufficient knowing that the identical mean value with the effective tensile modulus from FEM and standard deviation converged to less than 3% of the average value.

Model Output Calculation and Analysis

A defined square of elements was chosen to avoid edge effects (Jeong 2008). Strain values from all elements within the defined square were tracked (Fig 1). The effective elastic modulus for differently oriented strands was obtained by dividing the applied stress by the average resultant strain values over each element within the square. The deterministic FEM

Table 1. *Distribution types and parameters for material properties from Jeong et al (2009).*

Input variables	Average value	Fitted distribution	Theta	Scale	Shape
		- - - - E_L (GPa) - - -			
Earlywood 1 – 10	1.92	Weibull	0.077	2.049	3.410
Latewood 1 – 10	3.44	Weibull	1.699	1.947	1.697
Earlywood 11 – 20	2.48	Weibull	1.0	1.670	2.200
Latewood 11 – 20	5.09	Weibull	2.248	3.149	1.534
		- - - - υ_{LR} - - -			
Earlywood 1 – 10	0.49	Weibull	0	0.161	3.004
Latewood 1 – 10	0.59	Gamma	0	0.144	4.105
Earlywood 11 – 20	0.49	Gamma	0	0.144	3.429
Latewood 11 – 20	0.8	Weibull	0	0.841	2.359

models, including homogeneous models, produced one effective tensile MOE for each strand, whereas the SFEM models produced 1000 effective tensile MOE for each strand orientation.

Strain distributions were obtained from the deterministic FEM models including homogenous models, because the output values were calculated based on average input properties. Strain values were obtained from various positions along the line marked "path" in Fig 1. The path was located in the center of the strand (50 mm from both bottom and top) to minimize end effects.

One thousand effective tensile MOE values obtained from the SFEM model were correlated with the 1000 sets of stochastic input parameters generated from the input property distributions (Table 1). The Pearson correlation coefficient (r) was used to measure the correlation between the input and output parameters (Eq 1).

$$r = \frac{n(\sum XY) - (\sum [X](\sum [Y])]}{\sqrt{\left[n\sum X^2 - (\sum X)^2\right]\left[n\sum Y^2 - (\sum Y)^2\right]}} \quad (1)$$

where

r: Pearson correlation coefficient;
n: Number of samples;
X: Random input variable;
Y: Effective tensile MOE outputs; and
XY: Covariance between random input variable and tensile MOE output.

RESULTS AND DISCUSSION

Comparison of Experimental to Model Results

Table 2 shows the average experimental tensile MOE results for the differently oriented strands from growth ring numbers 1 – 10 and 11 – 20 and the current model results including the H model results with percentage difference comparisons from previous testing (Jeong 2008). Both the deterministic FEM and SFEM produced the same average results, which are reported here as FEM average values. The same average results were produced because the average material properties of earlywood and latewood were the same for the FEM and SFEM models regardless of different distributions of earlywood and latewood material properties. The SFEM model was used to analyze the distribution of outputs based on the distribution of inputs and the correlation between input and output parameters, which are discussed subsequently.

Comparing the experimental values with the homogeneous and FEM model results (Table 2), the FEM model results had better agreement with the experimental results over the range of strand orientations tested than the H model. Although RO and TO strands from growth ring numbers 1 – 10 were predicted best by the H model (–0.78 and 1.71% different, respectively), all other strand prediction results from the H models were greater than 20% different to a maximum of 36.1%. Predictions from the H model for the RO and TO strands from growth ring numbers 1 – 10 were very similar to the experimental results

Table 2. *Comparison of average tensile modulus of elasticity (MOE) from experimental and models.*

		Average tensile MOE (GPa)			Percent difference[a]	
Orientation	Growth ring numbers	Experimental[b]	Homogeneous	FEM[c]	Experimental vs homogeneous	Experimental vs FEM
Radial	1 – 10	2.41	2.43	2.43	–0.78%	–0.80%
Radial	11 – 20	2.75	3.35	3.36	–21.9%	–22.3%
Tangential	1 – 10	2.47	2.43	2.26	1.71%	8.57%
Tangential	11 – 20	2.53	3.35	3.02	–32.6%	–19.6%
Angled	1 – 10	1.97	2.43	2.12	–23.3%	–7.62%
Angled	11 – 20	2.46	3.35	2.80	–36.1%	–13.8%

[a] Percent difference = (experimental – model)/experimental × 100%.
[b] Experimental values were obtained from Jeong (2008).
[c] Deterministic FEM and SFEM average effective tensile MOE was identical.
FEM, finite element model; SFEM, stochastic finite element method.

because of the uniformity of strand placement and the smaller differences in the earlywood and latewood elastic properties from growth ring numbers 1 – 10 compared with the elastic properties from growth ring numbers 11 – 20.

The tensile MOE of the experimental vs FEM results for RO, TO, and AO strands from growth ring numbers 11 – 20 had higher percentage differences than did the strands from growth ring numbers 1 – 10. A higher ratio of latewood to earlywood MOE and a higher ratio of latewood to earlywood Poisson ratio may create slippage between earlywood and latewood within the strands. However, the current model assumed no slippage between the earlywood and latewood layers resulting in higher tensile MOE values predicted by the models.

For the prediction of the average effective tensile MOE for RO strands from the two growth ring numbers, the H and FEM models showed little change in percentage differences (Table 2). From the analogy of laminate theory, RO models experience a constant strain along the Y-axis. Because the input properties for the H model were applied using the rule of mixtures, the H models for RO strands showed a similar strain value obtained from the FEM models. However, the average effective tensile MOE from the TO and AO models was more highly influenced by the orientation and corresponding strain distribution. The H model did not represent the different orientation of earlywood and latewood in the TO and AO models, causing a higher percentage difference with the experimental results.

Strain Distribution from Different Strand Models

Figures 2 and 3 show the longitudinal Y-strain and transverse X-strain distribution along the path through the center of the strand models denoted in Fig 1 from the deterministic FEM. For the different strand models, earlywood and latewood bands changed position with the different orientations throughout the path. Typically, a smaller strain plateau indicated the latewood band and a larger strain plateau indicated the earlywood band.

Figure 2 shows the longitudinal Y-strain distribution of the strand models from the two growth ring positions. H and RO orientation models showed the same uniform strain distribution through the width. TO and AO models showed nonuniform Y-strain distribution because the grain orientation was not parallel to the loading direction. TO models showed a maximum value in strain near the edges, which decreased to a minimum value at the center. AO models showed the Y-strain distribution in earlywood was higher than latewood because the higher stiffness of latewood produced less strain at the same load level. All models showed a lower magnitude Y-strain distribution from growth ring numbers 11 – 20 compared with 1 – 10.

Figure 3 shows the transverse X-strain distributions of the strand models from the two growth ring positions. The H models showed uniform X-strain distribution through the width of the models. RO models showed a greater magnitude of negative strain in the latewood bands compared with earlywood bands because of higher latewood Poisson ratios (Table 1). This result may seem counterintuitive considering the higher tensile MOE of the latewood, but it illustrated the role of the Poisson ratio in the elastic behavior of strand materials. The TO models had the greatest negative strain of all models, which occurred near the edge of the model and decreased to the center because of the alignment direction of earlywood and latewood. The AO models showed a change in strain between earlywood and latewood bands with an overall decreasing strain toward the center. The strain distribution from growth ring numbers 11 – 20 showed a lower magnitude for all strand models than the strain distribution from 1 – 10.

The homogenous model produced similar strain distributions to the Y-strain radial orientation and produced good predictions of the effective tensile MOE of the RO 1 – 10 and TO 1 – 10 strands. However, the H model did not compare

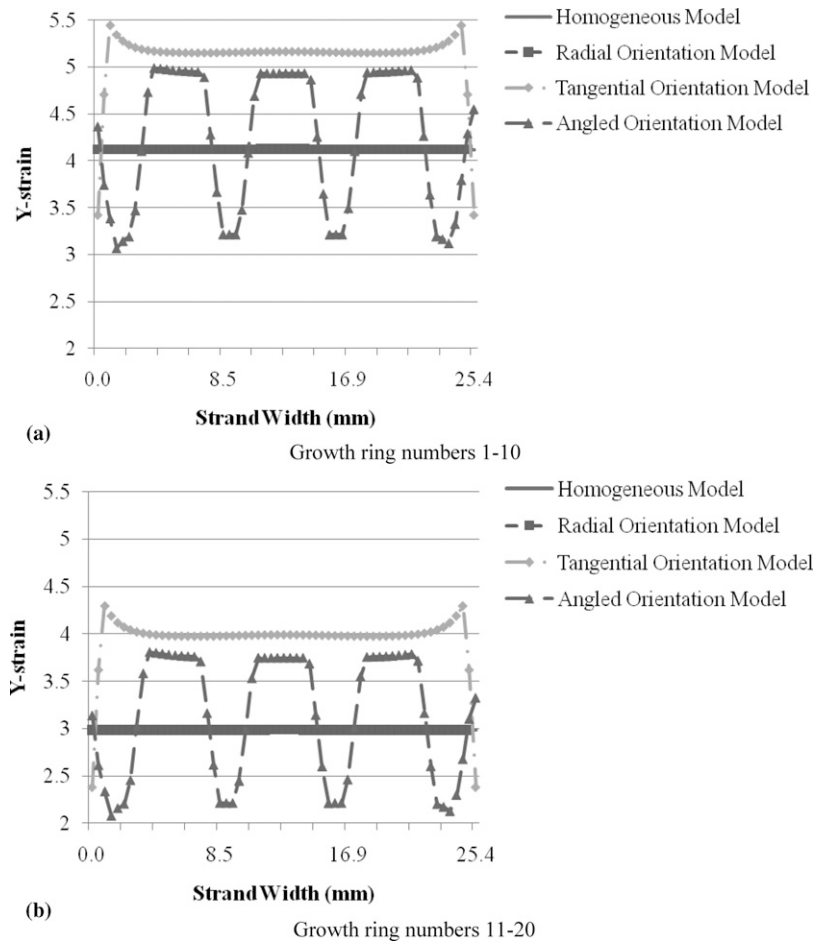

Figure 2. Y-strain distribution from simulation models. (a) Growth ring numbers 1 – 10; (b) growth ring numbers 11 – 20.

well with the strain distribution observed for the X-strain RO nor any of the TO or AO strain distributions. The assumption of homogeneity creating a uniform strain did not demonstrate the maximum values of local strain observed that are important to the failure analysis of the differently oriented strands (Jeong and Hindman 2009).

Statistical Distribution of the Effective Tensile Modulus of Elasticity

Figure 4 shows the cumulative probability of the effective tensile MOE of RO, TO, and AO from SFEM models and experimental testing from Jeong (2008). Thirty test results from the experimental tensile MOE results and 1000 simulation results from SFEM results were fitted in each graph in Fig 4. Kolmogorov-Smimov tests with a 95% confidence interval ($\alpha = 0.05$) showed that the comparison between experimental results and SFEM results was not significantly different (p-value 0.999 for RO 1 – 10, 0.973 for TO 1 – 10, 0.198 for TO 11 – 20, 0.855 for AO 1 – 10, 0.275 for AO 11 – 20), except for the comparison of RO strands from growth ring numbers 11 – 20 (p-value 0.001 for RO 11 – 20 comparison).

Several trends can be observed from Fig 4. The strands from growth ring numbers 1 – 10 always had a lower effective tensile MOE value than the 11 – 20 growth ring numbers. This result was expected based on previous research and the ear-

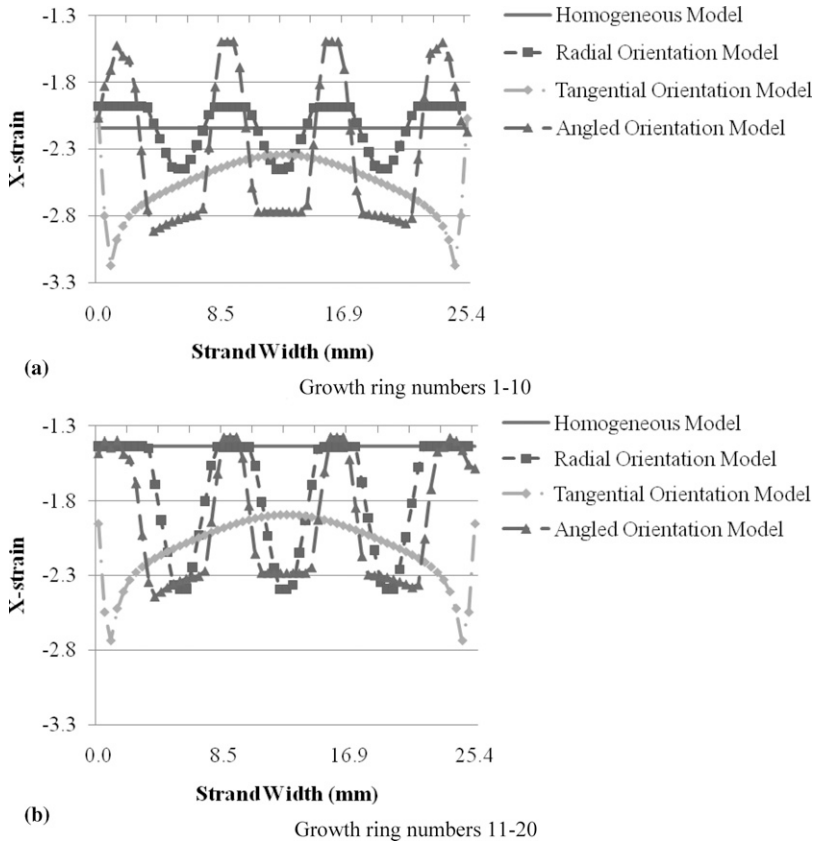

Figure 3. X-strain distribution from simulation models. (a) Growth ring numbers 1 – 10; (b) growth ring numbers 11 – 20.

lywood and latewood elastic properties from Table 1. Over the three different strand orientations, the difference in the 1 – 10 and 11 – 20 effective tensile MOE appeared to be reasonably consistent. The SFEM model results tended to predict higher effective tensile MOE values than the experimental results. For instance, the highest effective tensile MOE value of RO 11 – 20 from experimental testing was 3.48 GPa, whereas the highest value from the model was 5.29 GPa. The lowest effective tensile MOE value of TO 11 – 20 from experimental testing was 1.35 GPa, whereas the lowest effective tensile MOE value of TO 11 – 20 from the model was 1.53 GPa.

The model overprediction of the effective tensile MOE may be attributed to the assumptions used in the FEM and SFEM models. One assumption was that there is no slippage between the earlywood and latewood layers. A degree of slippage between the earlywood and latewood layers and within the intrarings would cause a lower effective tensile MOE value. RO strands from growth ring numbers 11 – 20 appear to be the most susceptible to the differential elastic behavior described. Because the loading direction is parallel to the earlywood and latewood orientation, these results show greater differences in elastic modulus and Poisson ratio between earlywood and latewood compared with the differences from growth ring numbers 1 – 10.

Sensitivity of Input Variables for the Effective Tensile Modulus of Elasticity of Differently Oriented Strand Models

Table 3 shows the sensitivity of input variables (tensile MOE and Poisson ratio for earlywood

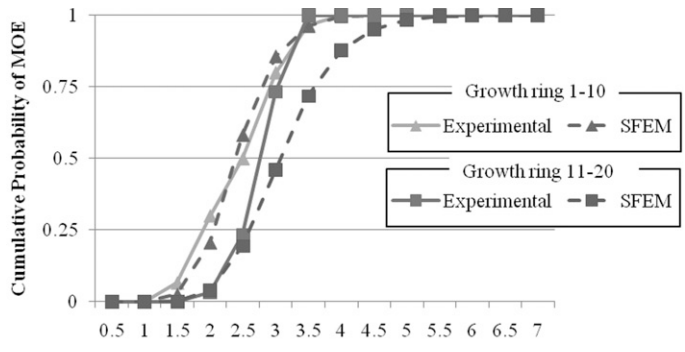

(a)

Comparison for tensile MOE of radial orientation strands from experimental and SFEM

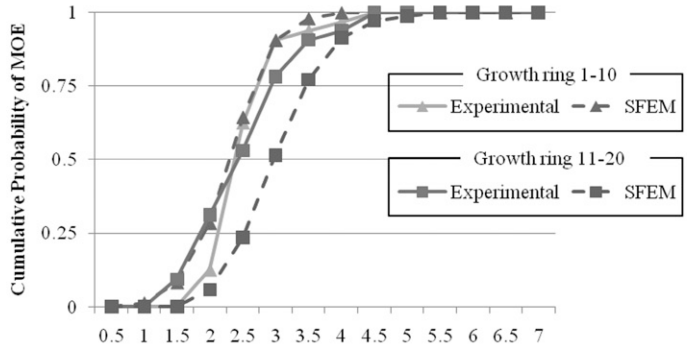

(b)

Comparison for tensile MOE of tangential orientation strands from experimental and SFEM

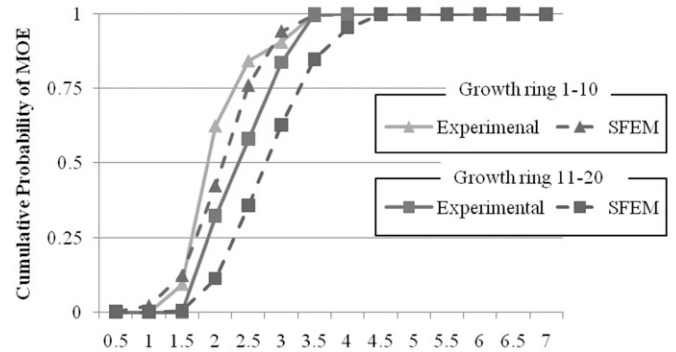

(c)

Comparison for tensile MOE of angled orientation strands from experimental and SFEM

Figure 4. Cumulative probability of tensile modulus of elasticity from experimental and stochastic finite element method; (a) radial orientation, (b) tangential orientation, (c) angled orientation.

and latewood from growth ring numbers 1 – 10 and 11 – 20) on the effective tensile MOE from the SFEM models. Bold numbers represent a strong correlation of Pearson linear correlation coefficient, defined as greater than 0.6, between an input variable and effective tensile MOE of strand models (Eq 1).

Effective tensile MOE of RO, TO, and AO strands was strongly correlated with earlywood

Table 3. *Sensitivity analysis of input variables on effective tensile modulus of elasticity (MOE) of differently oriented strands from growth ring numbers 1 – 10 and 11 – 20 showing the Pearson linear correlation.*

		Coefficient (r)[a]		
		Growth ring numbers 1 – 10		
Intrarings	Variables	Radial	Tangential	Angled
Earlywood 1 – 10	MOE	**0.734**	**0.916**	**0.952**
	Poisson ratio	0.410	0.551	0.598
Latewood 1 – 10	MOE	**0.662**	0.259	0.255
	Poisson ratio	0.571	0.168	0.194
		Growth ring numbers 11 – 20		
Intrarings	Variables	Radial	Tangential	Angled
Earlywood 11 – 20	MOE	**0.603**	**0.899**	**0.936**
	Poisson ratio	0.400	0.563	0.543
Latewood 11 – 20	MOE	**0.809**	0.385	0.269
	Poisson ratio	0.452	0.256	0.192

[a] Bold numbers represent a strong correlation between input and output.

tensile MOE, whereas only effective tensile MOE of RO strands was strongly correlated with latewood tensile MOE regardless of growth ring numbers. From the strain distributions associated with the differently oriented strands (Fig 2), increments of earlywood tensile MOE increased the effective tensile MOE of the TO and AO strands more than increments of latewood tensile MOE, whereas increments of latewood tensile MOE increased the effective tensile MOE of the RO strands more than increments of earlywood tensile MOE. Regardless of growth ring number and orientation, earlywood tensile MOE was a dominant factor that controlled effective tensile MOE of different orientations of wood strands.

Compared with RO strands, TO and AO strands had a higher correlation between earlywood Poisson ratio and the effective tensile MOE and lower correlation between latewood Poisson ratio and the effective tensile MOE. The correlation between Poisson ratio from earlywood and latewood and effective tensile MOE of differently oriented wood strands can be explained by different Y-strain distribution associated with X-strain distribution (Figs 2 and 3). From the superimposed Y-strain and X-strain distributions, RO strands had a higher Poisson ratio for latewood bands, whereas TO and AO strands had a higher Poisson ratio for earlywood bands. Poisson ratio can increase by increments of X-strain and/or decrements of Y-strain. The effective tensile MOE of RO strands had a positive correlation with Poisson ratio of latewood, whereas the effective tensile MOE of TO and AO strands had a positive correlation with Poisson ratio of earlywood. The sensitivity of the effective tensile MOE values to earlywood and latewood variables changed according to the growth ring number and orientation of strands.

CONCLUSIONS

Tensile properties of differently oriented wood strands were evaluated using deterministic FEM models and SFEM models. Whereas the deterministic FEM models used average material properties of earlywood and latewood from growth ring numbers 1 – 10 and 11 – 20, SFEM models used the distribution of the material properties. Although the homogeneous model predicted the average effective tensile MOE well for RO and TO strands from growth ring numbers 1 – 10, the physical strain distribution showed unrealistic behavior. Compared with the deterministic homogeneous model, deterministic layer FEM and SFEM models showed more realistic strain distribution and provided a good prediction of the average effective tensile MOE of the different orientation strands. Cumulative probability curves from experimental testing and SFEM models showed good agreement. Variation of effective tensile MOE from differently oriented strands

between experimental results (Jeong 2008) and SFEM results ranged 0.96 – 22.31%. From the sensitivity analysis, earlywood tensile MOE had an overall greater effect on effective tensile MOE of wood strands than other input parameters. Earlywood Poisson ratio had a greater effect on effective tensile MOE of TO and AO strands, whereas latewood Poisson ratio had a greater effect on effective tensile MOE of RO strands. SFEM models showed the capability of representing variation of material properties of differently oriented wood strands associated with earlywood and latewood variables.

REFERENCES

Clouston P (2007) Characterization and strength modeling of parallel-strand lumber. Holzforschung 61(4):394 – 399.

Clouston P, Lam F (2002) A stochastic plasticity approach to strength modeling of strand-based wood composites. Compos Sci Technol 62(10/11):1381 – 1395.

Cramer SM, Kretschmann DE, Lakes R, Schmidt T (2005) Earlywood and latewood elastic properties in loblolly pine. Holzforschung 59(5):531 – 538.

Groom LH, Mott L, Shaler S (2002) Mechanical properties of individual southern pine fibers. Part I. Determination and variability of stress-strain curves with respect to tree height and juvenility. Wood Fiber Sci 34(1):14 – 27.

Hindman DP, Lee JN (2007) Modeling wood strands as multi-layer composites: Bending and tension loads. Wood Fiber Sci 39(4):515 – 526.

Jeong GY (2005) Fracture behavior of wood plastic composite (WPC). Pp. 41 –81. MS Thesis, Louisiana State University, Baton Rouge, LA.

Jeong GY (2008) Tensile properties of loblolly pine strands using digital image correlation and stochastic finite element method. Pp. 99 – 138. PhD dissertation, Virginia Tech, Blacksburg, VA.

Jeong GY, Hindman DP (2009) Ultimate tensile strength of loblolly pine strands using stochastic finite element method. J Mater Sci 44(14):3824 – 3832.

Jeong GY, Zink-Sharp A, Hindman DP (2009) Tensile properties of earlywood and latewood from loblolly pine (*Pinus taeda*) using digital image correlation. Wood Fiber Sci 41(1):51 – 63.

Kleiber M, Hien T (1992) The stochastic finite element method: Basic perturbation technique and computer implementation. John Wiley and Sons, New York, NY.

Kretschmann DE, Cramer SM, Lakes R, Schmidt T (2006) Selected mesostructure properties in loblolly pine from Arkansas plantations. Pages 149 – 170 *in* DD Stokke and LH Groom, eds. Proc Characterization of the cellulosic cell wall, August 25 – 27, 2003. Wiley-Blackwell, Somerset, NJ.

Larson PR, Kretschmann DE, Clark A III, Isebrands JG (2001) Juvenile wood formation and properties in southern pine. Gen Tech Rep FPL-GTR-129. USDA For Prod Lab, Madison, WI.

Mott L, Groom LH, Shaler S (2002) Mechanical properties of individual southern pine fibers. Part II. Comparison of earlywood and latewood fibers with respect to tree height and juvenility. Wood Fiber Sci 34(2):221 – 237.

Wang YT, Lam F (1998) Computational modeling of material failure for parallel-aligned strand-based wood composites. Comp Mater Sci 11(3):157 – 165.